Microspheres Used in Liver Radioembolization

Subjects: Others

Contributor: Philippe D'ABADIE

Inert microspheres, labeled with several radionuclides, have been developed during the last two decades for the intra-arterial treatment of liver tumors, generally called Selective Intrahepatic radiotherapy (SIRT). The aim is to embolize microspheres into the hepatic capillaries, accessible through the hepatic artery, to deliver high levels of local radiation to primary (such as hepatocarcinoma, HCC) or secondary (metastases from several primary cancers, e.g., colorectal, melanoma, neuro-endocrine tumors) liver tumors. Several types of microspheres were designed as medical devices, using different vehicles (glass, resin, poly-lactic acid) and labeled with different radionuclides, 90Y and 166Ho.

liver radioembolization radiolabeled microspheres dosimetry

1. Introduction

Liver radioembolization (RE) is commonly used for the treatment of hepatocellular carcinoma and secondary liver malignancies. This treatment is performed by injection of radioactive microspheres in the liver artery after transarterial catheterization. Radioactive microspheres are trapped in the microvasculature (arterioles) of tumors and of the liver parenchyma. Unlike the liver parenchyma, where blood supply is almost obtained by the portal vein, liver tumors are preferentially vascularized by the liver arteries. This preferential perfusion allows us to achieve good targeting of hypervascularized tumors with a limited radiation of the non-tumoral liver [1]. The technique was initially developed using iodine-131 (^{131}I) Lipiodol, a radiolabeled ethiodized oil [2]. Thereafter, radiolabeled microspheres have emerged using Yttrium-90 (^{90}Y) and holmium-166 (^{166}Ho). These radionuclides emit beta radiations of high energy, resulting in a high delivery of energy to the tumors (absorbed doses) in the range of 100 to 1000 Gy [3]. In comparison, the total tumor dose is limited to a maximum of 70 Gy in external beam radiotherapy to avoid liver damage [4].

Three types of microspheres are commercially available: ^{90}Y-resin microspheres (Sir-Spheres®, Sirtex Medical Ltd., Sydney, Australia), ^{90}Y-glass microspheres (Therasphere®, Boston Scientific, Boston, MA, USA) and ^{166}Ho-poly-L-lactic acid (PLLA) microspheres (QuiremSpheres®, Quirem Medical B.V., Deventer, The Netherlands). Other microspheres have been used but did not reach the level of marketing authorization in Europe, e.g., ^{188}Re-microspheres [5].

2. Preparations and Labeling (Sir-Spheres®, Therasphere®, QuiremSpheres®)

SIR-Spheres® are cation exchange resin microspheres labeled with ^{90}Y phosphate. The resin is supplied as symmetrical microspheres ranging from 30 to 50 µm in diameter, made of sulphuric acid groups attached to a styrene divinylbenzene copolymer resin (Aminex 50W-X4, Bio-Rad, Hercules, CA, USA). First, stable yttrium oxide (III) (^{89}Y) is activated in a neutron beam to its radioisotope ^{90}Y according to the nuclear reaction ^{89}Y (n,γ) ^{90}Y. The radioactive yttria (Y2O3) is then dissolved in sulphuric acid. ^{90}Y is adsorbed onto the resin matrix by adding newly formed ^{90}Y sulphate solution to the aqueous slurry of microspheres. To immobilize and stably incorporate the ^{90}Y into the lattice, the radionuclide is precipitated as an insoluble phosphate salt by adding a tri-sodium phosphate solution. Finally, the microspheres are washed with a phosphate buffer solution and resuspended with water for injection [6].

The second commercially available product labeled with ^{90}Y is TheraSphere®. It consists of radioactive yttrium oxide-aluminosilicate glass microspheres. Inactive yttria is mixed with aluminum and silicone oxide. The resulting mixture is melted and stirred in a furnace at 1500 °C. The melt is then removed from the heat and rapidly quenched to a glass. The resultant glass frit is crushed to fine powder and filtered through a sieve. The powder is spheroidized by introducing it into a flame: the particles are melted and formed into spherical liquid drops by surface tension. The newly formed microspheres are quickly cooled and screened. The 20- to 30-µm fraction is rinsed and dried. The ^{89}Y embedded glass microspheres are eventually activated by neutron bombardment to the radioisotope ^{90}Y [7][8][9].

QuiremSpheres® are poly-L-lactic acid (PLLA) microspheres labeled with ^{166}Ho. The microspheres are synthesized by the solvent-evaporation technique. First, non-radioactive ^{165}Ho is complexed with acetylacetonate. Complex ^{165}Ho-acetylacetonate is then incorporated into the PLLA matrix by adding ^{165}Ho-actylacetonate and poly-L-lactic acid to a continuously stirred chloroform solution. The resulting solution is then added to an aqueous polyvinyl alcohol solution and stirred until complete evaporation of the chloroform. The newly formed ^{165}Ho-loaded microspheres are collected by centrifugation, washed and fractionated according to their size. The 20- to 50-µm fraction is dried and packed in polyethylene vials. Finally, ^{165}Ho is activated to ^{166}Ho in a nuclear reactor by neutron irradiation with a thermal neutron flux of 5×10^{12} cm^{-2} s^{-1} ($^{165}Ho + n \rightarrow {}^{166}Ho$, cross section 64 barn) [10][11][12]. The final product contains 19% (w/w) holmium (essentially stable which is of interest in view of the paramagnetic properties of ^{165}Ho, see paragraph 2) and a maximum ^{166}Ho specific activity per microsphere of 450 Bq [13]. QuiremSpheres® is supplied as a ready-to-use, tailored dose: the dispatched activity is patient-specific and matches the activity at treatment time as ordered by the customer. There is no need for patient-dose preparation on-site [14].

3. Radionuclide Properties and Clinical Applications

Table 1 summarizes the main physical characteristics of ^{90}Y and ^{166}Ho radionuclides.

Table 1. Physical characteristics of radionuclides.

	Labeled Microspheres	Half-Life	Beta Emission (E. Max)	Range of Beta Radiation	Other Emissions
Yttrium-90 (^{90}Y)	Resin or glass	2.7 days	2.28 MeV	Mean: 2.5 mm (Max: 11 mm)	Positron (32×10^{-6})
Holmium-166 (^{166}Ho)	Poly (L-Lactic acid)	1.1 day	1.77 MeV (49%), 1.86 MeV (50%)	Mean: 2.5 mm (Max: 8.7 mm)	Gamma (6.7%)

These beta particles generate free radical species in the presence of oxygen inducing DNA breaks and cell killing. Many factors influence the killing efficacy, and particularly the rate of beta particles emission (correlated to half-life) and the number of beta particles (correlated to the radioactive activity) [15]. The biological effect of radiations is demonstrated by the absorbed dose (Gy), defined by the energy (J) deposited per mass of tissue or tumor (kg). This absorbed dose is directly correlated to the cell survival fraction and tumor response [16].

The precise localization of these beta particles in the tumor is also an important factor for tumor response. Indeed, the very short range of beta emission (few millimeters) induce a biologic effect only in the neighborhood of the beta particles and consequently, their distribution in the tumor must be the as homogeneous as possible for killing a maximum of cells and induce a tumor response [17].

These radionuclides have also the ability to be detected by nuclear imaging systems. An accurate detection is important for evaluating the distribution in the targeted tissues and for a quantitative assessment of the dose deposition. Beta particles induce interactions with the surrounding tissues and generate a continuous spectrum of X-ray photons known as bremsstrahlung.

4. Radioactive Microspheres Properties

^{90}Y-resin, ^{90}Y-glass and ^{166}Ho-poly-L-lactic-acid [PLLA] microspheres differ from their physical characteristics, summarized in **Table 2** [7][18]. Globally, all three devices have a similar diameter around 30 µm, but some differences appear in the size spectrum distribution (**Figure 1**). MAA particles have a significantly lower size (mean: 15 µm).

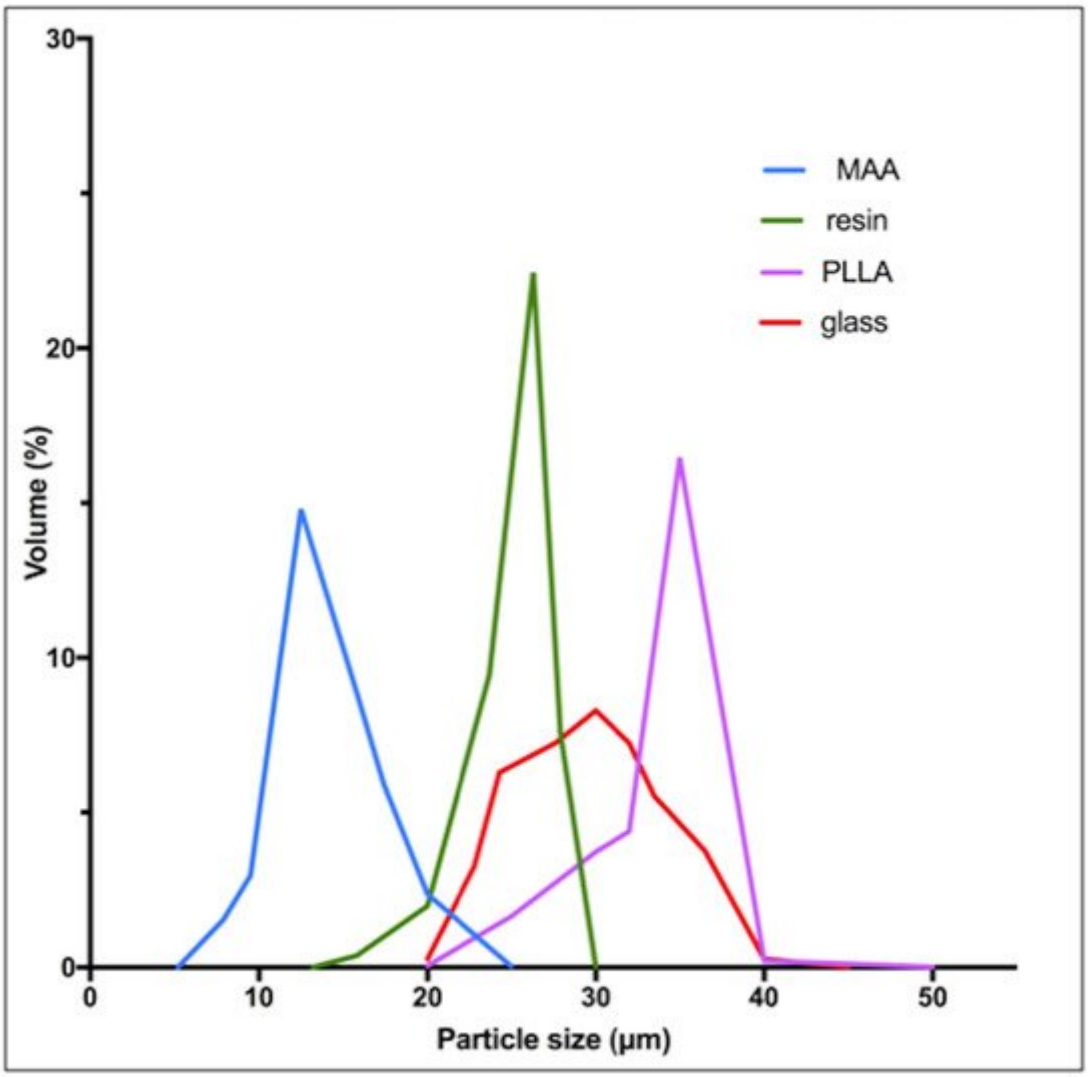

Figure 1. Particle size distribution for resin, glass, PLLA microspheres and MAA particles. **Figure 1** was made by rescaling graphs derived from the analyses of Bakker et al. [19], Bult W. [20] and Gupta et al. using iron labeled glass microspheres [21].

Resin and PLLA microspheres have a density comparable to blood (1.06 g/mL). Glass microspheres have a higher density (3.3 g/mL) three-fold more than blood. Regarding the specific activity per microsphere and the number of microspheres injected, resin, glass and PLLA microspheres differ highly (**Table 2**).

Table 2. Physical characteristics of radioactive microspheres.

Microspheres	Diameter (Mean)	Density	Approximative Number of Micro-Spheres Per GBq *	Activity Per Microsphere
^{90}Y-Resin	32 µm	1.6 g/mL	13×10^6	50 Bq
^{90}Y-Glass	25 µm	3.3 g/mL	0.4×10^6	2500 Bq

Microspheres	Diameter (Mean)	Density	Approximative Number of Micro-Spheres Per GBq *	Activity Per Microsphere
^{166}Ho-PLLA	30 µm	1.4 g/mL	10×10^6	450 Bq

* On the day of calibration (approximately). PLLA: poly-(L-lactic-acid).

5. Impact at a Microscopic Level-Microdosimetry

Due to their physical differences, these types of microspheres have a different distribution into the liver at the microscopic level, which results in major differences in local absorbed doses.

Contrarily to external radiotherapy, the absorbed dose distribution is heterogeneous in liver radioembolization resulting from the heterogeneous microsphere distribution at a microscopic level [22][23]. Moreover, due to their physical differences, the distribution of the absorbed dose into the liver is very different between the types of microspheres.

^{90}Y-resin, ^{90}Y-glass and ^{166}Ho-PLLA microspheres have a similar diameter permitting us to similarly reach the microvasculature of tumors. The higher density of glass microspheres (**Table 2**) does not have a significant impact in the microsphere distribution compared to resin microspheres, as demonstrated by an experimental model of the hepatic vasculature [24].

The main differences between microspheres are the specific activity per sphere and the number of injected microspheres during a treatment. Glass microspheres are especially highly radioactive (2500 Bq) and in limited number compared to others.

In a very interesting in-vivo study in pigs, Pasciak et al. confirmed in-vivo correlation between the number of injected microspheres and the degree of homogeneity of the absorbed dose at a microscopic level [25]. In this study, four pigs received lobar infusions of ^{90}Y glass microspheres with an activity reaching a similar target liver dose of 50 Gy. In each pig, the injected glass microspheres differ in specific activity and number (from 1532 Bq/microsphere & 610 microspheres/mL of tissue to 70 Bq/microsphere & 15,555 microspheres/mL of tissue), as illustrated in **Figure 2**.

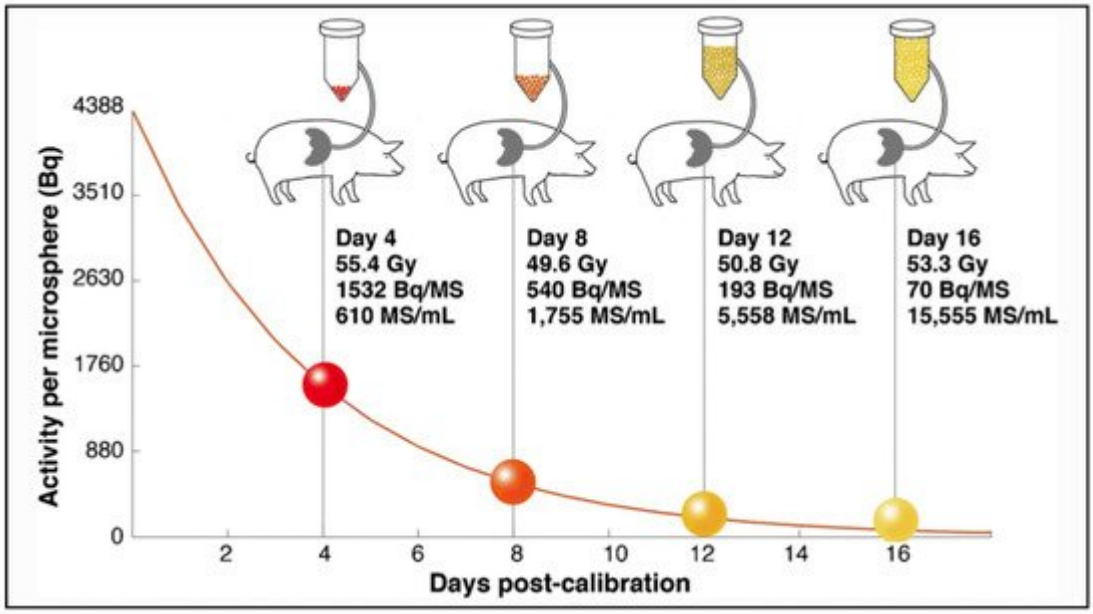

Figure 2. Amount of glass microspheres injected in pig livers as a function of time from microsphere calibration (4, 8, 12 or 16 days), resulting in spheres of different specific activity and concentrations. Reprinted from European journal of nuclear medicine and molecular imaging with permission of Springer Nature (Eur. J. Nucl. Med. Mol. Imaging 2020, 47, 816–827).

The analysis of the microdosimetry data demonstrated important differences in absorbed doses deposition at a microscopic level. Each pig received the same average dose of 50 Gy, but the distribution at a microscopic level was clearly different, being very inhomogeneous when the number of microspheres was lower. The percentage of the non-target liver receiving at least a potentially toxic dose of 40 Gy was only 24% for microspheres in relatively small number (e.g., 610 microspheres/mL of tissue) and 53% using more numerous microspheres (e.g., 15,555 microspheres/mL of tissue). This effect is well illustrated in **Figure 3**.

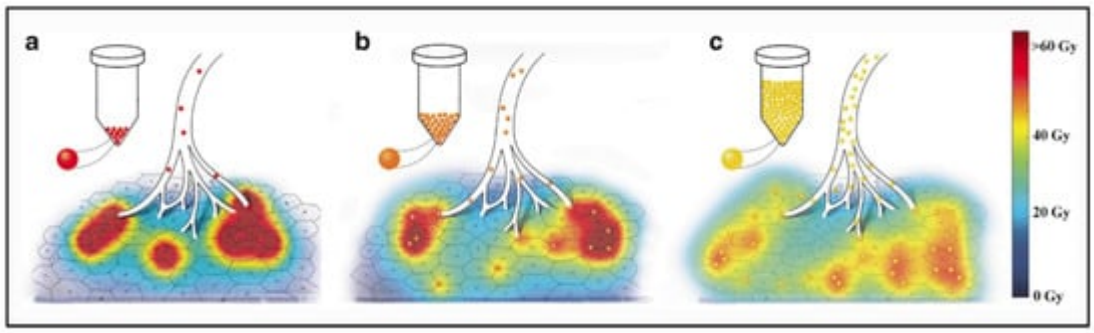

Figure 3. Artistic rendering of microscopic microsphere deposition at day 4 post-calibration (**a**), 8 post-calibration (**b**) and 12 post-calibration (**c**). Increased homogeneity of absorbed dose is apparent for glass microspheres injected at day 12 post-calibration (e.g., 193 Bq/microsphere, 5558 microspheres/mL). The proportion of the liver receiving a dose higher or equal to 40 Gy (red and yellow colors) was higher for glass microspheres injected at day 12 post-calibration (**c**). Reprinted from European journal of nuclear medicine and molecular imaging with permission of Springer Nature (Eur. J. Nucl. Med. Mol. Imaging 2020, 47, 816–827).

Using microspheres in limited number induces a more heterogeneous liver distribution, but also permits it to be less toxic, avoiding reaching a toxic dose in a large part of the normal liver. These dosimetric concepts could be extrapolated to any type of microspheres, in order to evaluate to what extent the number of microspheres and their specific activity can influence the efficacy and toxicity of liver radioembolization.

^{90}Y- resin and^{166}Ho- PLLA microspheres could have an embolic effect because a high number of particles are injected in the liver arterial tree (**Table 2**). However, this effect may be very limited in particular because they have a very small size, permitting to reach the terminal microvasculature [26].

6. Impact at a Macroscopic Level-Clinical Effects

Physical characteristics of the radioactive microspheres explain also their different toxicity and efficacy profiles. Regarding PLLA microspheres (Quirem Spheres®), more data are needed to evaluate and compare its efficiency and toxicity.

Regarding toxicity, an excessive irradiation of the healthy liver can induce a severe and potentially life-threatening complication: radioembolization induced liver disease (REILD) with an incidence rate inferior to 4% [26]. It is described by a sinusoidal obstruction syndrome and by a liver damage within 3 months after RE, in absence of tumor progression [27]. This complication tends to occur especially when a large volume of liver parenchyma is exposed to radiations. Other risk factors include a recent exposition to chemotherapy and underlying cirrhosis [28]. In external beam radiotherapy (EBRT), this complication occurs with whole liver doses of 30–35 Gy [29]. The tolerance is higher in RE, 40–50 Gy for resin microspheres and 90 Gy with glass microspheres [30][31][32]. A pre-clinical study in pigs with administration of PLLA microspheres demonstrates no toxicity with absorbed doses over 100 Gy. In human studies in phase 1 and 2, the whole liver absorbed dose was limited to 60 Gy and was not associated with any liver toxicity [33][34]. The homogeneity of the dose distribution explains the relative lower liver dose tolerability of external radiotherapy. To the contrary, a large heterogeneity of the dose distribution appears in RE, and a relative less proportion of liver parenchyma receives a toxic dose (i.e., 30–35 Gy). As described by Pasciak et al. [25], this liver dose heterogeneity is directly correlated to the number of microspheres injected in the liver. This characteristic could explain why the tolerable dose is significantly higher when a relatively small number of radioactive microspheres are injected into the liver (**Table 2**).

The ^{90}Y beta range being sub-centimetric, the result is that, contrary to EBRT, the absorbed dose itself is highly heterogeneous. As a consequence, for an absorbed dose of 40 Gy, a sufficient fraction of lobules experienced sub-lethal dose in TARE and can repopulate the liver pool. Estimation of this fraction by Monte Carlo simulations explains the difference between the maximal safe absorbed dose between glass and resin spheres radioembolization, as well as EBRT [35].

Previous data demonstrated a continuous relationship, a sigmoid correlation, between the tumor absorbed dose and the radiological response [31][36]. HCC patients treated with resin microspheres had better disease control and overall survival when tumor absorbed doses were above 100 Gy. HCC patients treated with glass microspheres

also had a better outcome with a tumor-absorbed dose of at least 205 Gy [37][38]. For colorectal metastases, a dose response relationship was also demonstrated with the three types of microspheres. A significant metabolic response was achieved with a tumor cutoff dose of 50–60 Gy with resin microspheres [39][40], 139 Gy using glass microspheres [41] and 90 Gy using PLLA microspheres [42]. Then, to be efficient, the tumor absorbed dose cutoff is approximately twice with glass microspheres as compared to resin microspheres. A recent comparison of patients treated with glass and resin microspheres demonstrated similar outcome using a tumor dose cutoff of 61 Gy with resin microspheres and 118 Gy with glass microspheres [43]. But interestingly, the analysis of the tumor dose at a microscopic level did not demonstrate a two-fold difference between both types of microspheres. Indeed, patients treated with glass or resin microspheres achieved similar outcome with the same minimal dose in most of the tumor volume. A minimum dose of 40 Gy in 66% of the tumor volume was associated with similar PFS and OS with both types of microspheres. The tumor dose distribution can be accurately studied with ^{90}Y PET/CT using dose volume histogram (DVH). **Figure 4** demonstrates examples of HCC tumors treated with glass microspheres with similar mean absorbed doses, but wide differences in intratumoral dose distributions.

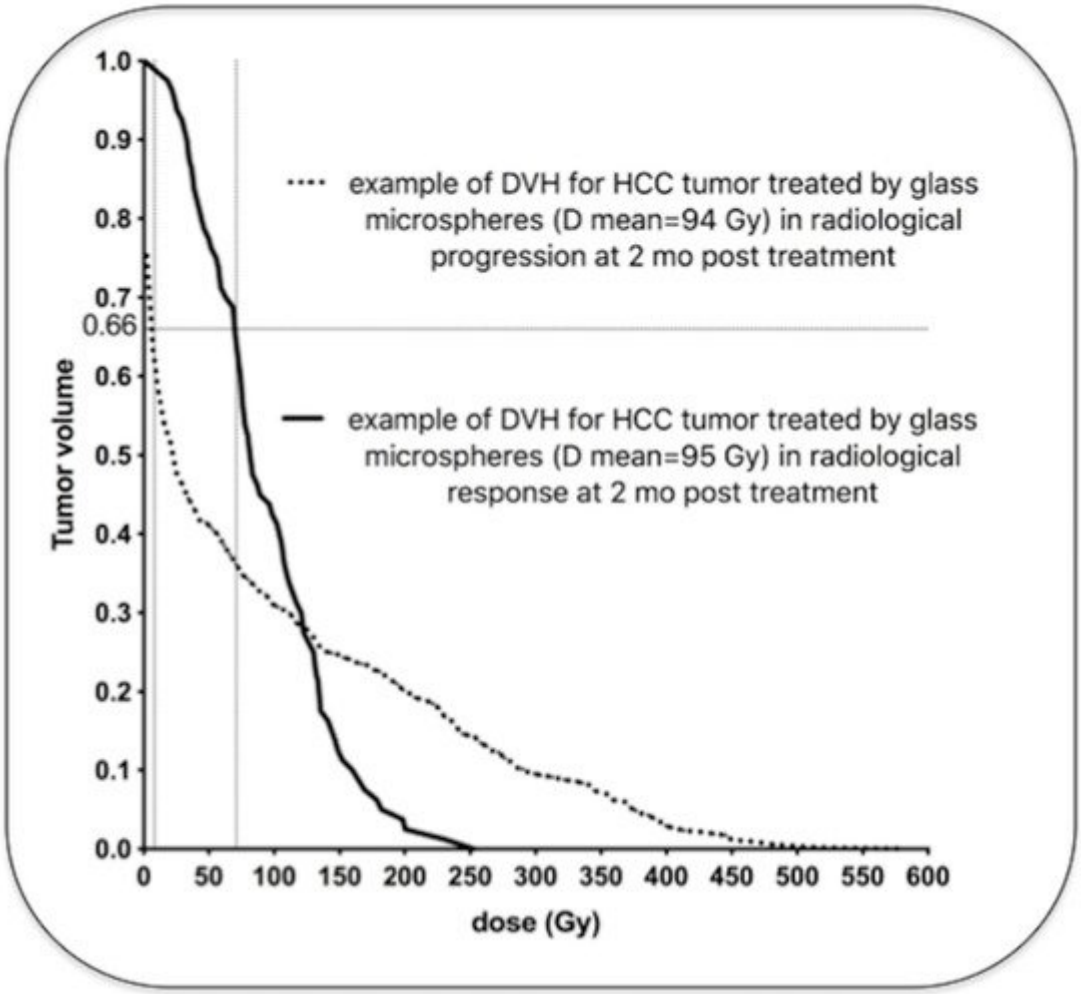

Figure 4. Examples of two HCC tumors treated with glass microspheres with similar mean absorbed doses (94 and 95 Gy) but very different dose distributions (personal data). One tumor (dotted line) received a very low dose in a large part of the tumor volume (more than 5 Gy in 66% of the tumor volume), and was in radiological progression two months later. The other tumor (solid line) received a high dose in a large part of the tumor volume (more than

69 Gy in 66% of the tumor volume) and was in radiological response two months later. Note that the cluster with the highest local dose was found in the non-responding tumor (>500 Gy) because of the major heterogeneous distribution.

References

1. Lewandowski, R.J.; Salem, R. Yttrium-90 radioembolization of hepatocellular carcinoma and metastatic disease to the liver. Semin. Interv. Radiol. 2006, 23, 64–72.
2. Giammarile, F.; Bodei, L.; Chiesa, C.; Flux, G.; Forrer, F.; Kraeber-Bodere, F.; Brans, B.; Lambert, B.; Konijnenberg, M.; Borson-Chazot, F.; et al. EANM procedure guideline for the treatment of liver cancer and liver metastases with intra-arterial radioactive compounds. Eur. J. Nucl. Med. Mol. Imaging 2011, 38, 1393–1406.
3. Kennedy, A.S.; Nutting, C.; Coldwell, D.; Gaiser, J.; Drachenberg, C. Pathologic response and microdosimetry of 90Y microspheres in man: Review of four explanted whole livers. Int. J. Radiat. Oncol. 2004, 60, 1552–1563.
4. Kennedy, A. Radioembolization of hepatic tumors. J. Gastrointest. Oncol 2014, 5, 178–189.
5. Lambert, B.; Bacher, K.; Defreyne, L. Rhenium-188 based radiopharmaceuticals for treatment of liver tumours. Q. J. Nucl. Med. Mol. Imaging 2009, 53, 305–310.
6. Gray, B.N. Polymer Based Radionuclide Containing Particulate Material. Patent No. WO2002034300A1, 2 May 2002.
7. Westcott, M.A.; Coldwell, D.M.; Liu, D.M.; Zikria, J.F. The development, commercialization, and clinical context of yttrium-90 radiolabeled resin and glass microspheres. Adv. Radiat. Oncol. 2016, 1, 351–364.
8. Day, D.; Ehrhardt, G. Glass Microspheres. U.S. Patent 4,789,501, 6 December 1986.
9. Therasphere, Products Pecifications. Available online: (accessed on 13 May 2021).
10. Nijsen, J.; van Steenbergen, M.; Kooijman, H.; Talsma, H.; Kroon-Batenburg, L.; van de Weert, M.; van Rijk, P.; de Witte, A.; Schip, A.V.H.; Hennink, W. Characterization of poly(l-lactic acid) microspheres loaded with holmium acetylacetonate. Biomaterials 2001, 22, 3073–3081.
11. Nijsen, J.F.; Zonnenberg, B.A.; Woittiez, J.R.; Rook, D.W.; Swildens-van Woudenberg, I.A.; van Rijk, P.P.; van het Schip, A.D. Holmium-166 poly lactic acid microspheres applicable for intra-arterial radionuclide therapy of hepatic malignancies: Effects of preparation and neutron activation techniques. Eur. J. Nucl. Med. 1999, 26, 699–704.
12. Zielhuis, S.; Nijsen, J.; de Roos, R.; Krijger, G.; van Rijk, P.; Hennink, W.; Schip, A.V.H. Production of GMP-grade radioactive holmium loaded poly(l-lactic acid) microspheres for clinical application.

Int. J. Pharm. 2006, 311, 69–74.

13. Arranja, A.; Hennink, W.; Chassagne, C.; Denkova, A.; Nijsen, J. Preparation and characterization of inorganic radioactive holmium-166 microspheres for internal radionuclide therapy. Mater. Sci. Eng. C 2020, 106, 110244.
14. QuiremSpheres. Instruction for Use. Available online: (accessed on 5 October 2020).
15. Zhao, J.; Zhou, M.; Li, C. Synthetic nanoparticles for delivery of radioisotopes and radiosensitizers in cancer therapy. Cancer Nanotechnol. 2016, 7, 1–23.
16. Brans, B.; Bodei, L.; Giammarile, F.; Linden, O.; Luster, M.; Oyen, W.J.G.; Tennvall, J. Clinical radionuclide therapy dosimetry: The quest for the "Holy Gray". Eur. J. Nucl. Med. Mol. Imaging 2007, 34, 772–786.
17. Sofou, S. Radionuclide carriers for targeting of cancer. Int. J. Nanomed. 2008, 3, 181–199.
18. Vente, M.A.; Nijsen, J.F.; de Wit, T.C.; Seppenwoolde, J.H.; Krijger, G.C.; Seevinck, P.R.; Huisman, A.; Zonnenberg, B.A.; van den Ingh, T.S.; van het Schip, A.D. Clinical effects of transcatheter hepatic arterial embolization with holmium-166 poly (L-lactic acid) microspheres in healthy pigs. Eur. J. Nucl. Med. Mol. Imaging 2008, 35, 1259–1271.
19. Bakker, R.C.; de Roos, R.; Ververs, F.T.; Lam, M.G.; van der Lee, M.K.; Zonnenberg, B.A.; Krijger, G.C. Blood and urine analyses after radioembolization of liver malignancies with [166Ho]Ho-acetylacetonate-poly(l-lactic acid) microspheres. Nucl. Med. Biol. 2019, 71, 11–18.
20. Bult, W. Holmium Microparticles for Intratumoral Radioablation. Ph.D. Thesis, Utrecht University, Utrecht, The Netherlands, 2010.
21. Gupta, T.; Virmani, S.; Neidt, T.M.; Szolc-Kowalska, B.; Sato, K.T.; Ryu, R.K.; Lewandowski, R.J.; Gates, V.L.; Woloschak, G.E.; Salem, R.; et al. MR tracking of iron-labeled glass radioembolization microspheres during transcatheter delivery to rabbit VX2 liver tumors: Feasibility study. Radiology 2008, 249, 845–854.
22. Hogberg, J.; Rizell, M.; Hultborn, R.; Svensson, J.; Henrikson, O.; Molne, J.; Gjertsson, P.; Bernhardt, P. Increased absorbed liver dose in Selective Internal Radiation Therapy (SIRT) correlates with increased sphere-cluster frequency and absorbed dose inhomogeneity. EJNMMI Phys. 2015, 2, 10.
23. Hogberg, J.; Rizell, M.; Hultborn, R.; Svensson, J.; Henrikson, O.; Molne, J.; Gjertsson, P.; Bernhardt, P. Heterogeneity of microsphere distribution in resected liver and tumour tissue following selective intrahepatic radiotherapy. EJNMMI Res. 2014, 4, 48.
24. Caine, M.; McCafferty, M.S.; McGhee, S.; Garcia, P.; Mullett, W.M.; Zhang, X.; Hill, M.; Dreher, M.R.; Lewis, A.L. Impact of Yttrium-90 Microsphere Density, Flow Dynamics, and Administration

Technique on Spatial Distribution: Analysis Using an In Vitro Model. J. Vasc. Interv. Radiol. 2017, 28, 260–268.e2.

25. Pasciak, A.S.; Abiola, G.; Liddell, R.P.; Crookston, N.; Besharati, S.; Donahue, D.; Thompson, R.E.; Frey, E.; Anders, R.A.; Dreher, M.R.; et al. The number of microspheres in Y90 radioembolization directly affects normal tissue radiation exposure. Eur. J. Nucl. Med. Mol. Imaging 2020, 47, 816–827.
26. Riaz, A.; Awais, R.; Salem, R. Side effects of yttrium-90 radioembolization. Front. Oncol. 2014, 4, 198.
27. Braat, A.J.; Smits, M.L.; Braat, M.N.; van den Hoven, A.F.; Prince, J.F.; de Jong, H.W.; van den Bosch, M.A.; Lam, M.G. 90Y Hepatic Radioembolization: An Update on Current Practice and Recent Developments. J. Nucl. Med. 2015, 56, 1079–1087.
28. Gil-Alzugaray, B.; Chopitea, A.; Inarrairaegui, M.; Bilbao, J.I.; Rodriguez-Fraile, M.; Rodriguez, J.; Benito, A.; Dominguez, I.; D'Avola, D.; Herrero, J.I.; et al. Prognostic factors and prevention of radioembolization-induced liver disease. Hepatology 2013, 57, 1078–1087.
29. Koay, E.J.; Owen, D.; Das, P. Radiation-Induced Liver Disease and Modern Radiotherapy. Semin. Radiat. Oncol. 2018, 28, 321–331.
30. Cremonesi, M.; Ferrari, M.; Bartolomei, M.; Orsi, F.; Bonomo, G.; Arico, D.; Mallia, A.; De Cicco, C.; Pedroli, G.; Paganelli, G. Radioembolisation with 90Y-microspheres: Dosimetric and radiobiological investigation for multi-cycle treatment. Eur. J. Nucl. Med. Mol. Imaging 2008, 35, 2088–2096.
31. Strigari, L.; Sciuto, R.; Rea, S.; Carpanese, L.; Pizzi, G.; Soriani, A.; Iaccarino, G.; Benassi, M.; Ettorre, G.M.; Maini, C.L. Efficacy and toxicity related to treatment of hepatocellular carcinoma with 90Y-SIR spheres: Radiobiologic considerations. J. Nucl. Med. 2010, 51, 1377–1385.
32. Chiesa, C.; Mira, M.; Bhoori, S.; Bormolini, G.; Maccauro, M.; Spreafico, C.; Cascella, T.; Cavallo, A.; De Nile, M.C.; Mazzaglia, S.; et al. Radioembolization of hepatocarcinoma with 90Y glass microspheres: Treatment optimization using the dose-toxicity relationship. Eur. J. Nucl. Med. Mol. Imaging 2020, 47, 3018–3032.
33. Prince, J.F.; van den Bosch, M.; Nijsen, J.F.W.; Smits, M.L.J.; van den Hoven, A.F.; Nikolakopoulos, S.; Wessels, F.J.; Bruijnen, R.C.G.; Braat, M.; Zonnenberg, B.A.; et al. Efficacy of Radioembolization with 166Ho-Microspheres in Salvage Patients with Liver Metastases: A Phase 2 Study. J. Nucl. Med. 2018, 59, 582–588.
34. Smits, M.L.; Nijsen, J.F.; van den Bosch, M.A.; Lam, M.G.; Vente, M.A.; Mali, W.P.; van Het Schip, A.D.; Zonnenberg, B.A. Holmium-166 radioembolisation in patients with unresectable, chemorefractory liver metastases (HEPAR trial): A phase 1, dose-escalation study. Lancet Oncol. 2012, 13, 1025–1034.

35. Walrand, S.; Hesse, M.; Jamar, F.; Lhommel, R. A hepatic dose-toxicity model opening the way toward individualized radioembolization planning. J. Nucl. Med. 2014, 55, 1317–1322.
36. Hermann, A.L.; Dieudonne, A.; Ronot, M.; Sanchez, M.; Pereira, H.; Chatellier, G.; Garin, E.; Castera, L.; Lebtahi, R.; Vilgrain, V.; et al. Relationship of Tumor Radiation-absorbed Dose to Survival and Response in Hepatocellular Carcinoma Treated with Transarterial Radioembolization with 90Y in the SARAH Study. Radiology 2020, 296, 673–684.
37. Garin, E.; Lenoir, L.; Edeline, J.; Laffont, S.; Mesbah, H.; Poree, P.; Sulpice, L.; Boudjema, K.; Mesbah, M.; Guillygomarc'h, A.; et al. Boosted selective internal radiation therapy with 90Y-loaded glass microspheres (B-SIRT) for hepatocellular carcinoma patients: A new personalized promising concept. Eur. J. Nucl. Med. Mol. Imaging 2013, 40, 1057–1068.
38. Garin, E.; Tselikas, L.; Guiu, B.; Chalaye, J.; Edeline, J.; de Baere, T.; Assenat, E.; Tacher, V.; Robert, C.; Terroir-Cassou-Mounat, M.; et al. Personalised versus standard dosimetry approach of selective internal radiation therapy in patients with locally advanced hepatocellular carcinoma (DOSISPHERE-01): A randomised, multicentre, open-label phase 2 trial. Lancet Gastroenterol. Hepatol. 2021, 6, 17–29.
39. Van den Hoven, A.F.; Rosenbaum, C.E.; Elias, S.G.; de Jong, H.W.; Koopman, M.; Verkooijen, H.M.; Alavi, A.; van den Bosch, M.A.; Lam, M.G. Insights into the Dose-Response Relationship of Radioembolization with Resin 90Y-Microspheres: A Prospective Cohort Study in Patients with Colorectal Cancer Liver Metastases. J. Nucl. Med. 2016, 57, 1014–1019.
40. Willowson, K.P.; Hayes, A.R.; Chan, D.L.H.; Tapner, M.; Bernard, E.J.; Maher, R.; Pavlakis, N.; Clarke, S.J.; Bailey, D.L. Clinical and imaging-based prognostic factors in radioembolisation of liver metastases from colorectal cancer: A retrospective exploratory analysis. EJNMMI Res. 2017, 7, 46.
41. Alsultan, A.A.; van Roekel, C.; Barentsz, M.W.; Smits, M.L.J.; Kunnen, B.; Koopman, M.; Bruijnen, R.C.G.; de Keizer, B.; Lam, M. Dose-response and dose-toxicity relationships for yttrium-90 glass radioembolization in patients with colorectal cancer liver metastases. J. Nucl. Med. 2021.
42. Van Roekel, C.; Bastiaannet, R.; Smits, M.L.J.; Bruijnen, R.C.; Braat, A.; de Jong, H.; Elias, S.G.; Lam, M. Dose-Effect Relationships of 166Ho Radioembolization in Colorectal Cancer. J. Nucl. Med. 2021, 62, 272–279.
43. D'Abadie, P.; Walrand, S.; Hesse, M.; Annet, L.; Borbath, I.; Van den Eynde, M.; Lhommel, R.; Jamar, F. Prediction of tumor response and patient outcome after radioembolization of hepatocellular carcinoma using 90Y-PET-computed tomography dosimetry. Nucl. Med. Commun. 2021.